Coordinate-free description of corrugated flames with realistic density drop at the front

Vitaly Bychkov,[1] Maxim Zaytsev,[1,2] and V'yacheslav Akkerman[1,2]
[1]*Institute of Physics, Umeå University, SE 901 87 Umeå, Sweden*
[2]*Moscow Institute of Physics and Technology, 141 700 Dolgoprudny, Russia*
(Received 4 April 2003; published 26 August 2003)

The complete set of hydrodynamic equations for a corrugated flame front is reduced to a system of coordinate-free equations at the front using the fact that the vorticity effects remain relatively weak even for corrugated flames. It is demonstrated how small but finite flame thickness may be taken into account in the equations. Similar equations are obtained for turbulent burning in the flamelet regime. The equations for a turbulent corrugated flame are consistent with the Taylor hypothesis of ''stationary'' external turbulence.

DOI: 10.1103/PhysRevE.68.026312 PACS number(s): 47.20.−k, 47.27.−i, 82.33.Vx

I. INTRODUCTION

One of the most difficult problems of premixed combustion modeling is the huge difference in length scales involved in the burning process. While the characteristic length scale of the hydrodynamic flow varies from $5-10$ cm (car engines) to several meters (turbine combustors), the flame thickness is typically much smaller $L_f=(10^{-4}-10^{-3})$ cm, and the zone of active reaction is even thinner $0.1L_f$ [1]. No computer can resolve all these length scales at present, and therefore one of the main tasks of combustion science is to create a reliable model of burning, both turbulent and laminar. The problem may be simplified considerably, if one manages to reduce the whole system of combustion equations to a single equation for the flame front position. This is possible, for example, for a turbulent flame in the artificial case of zero density variation across the flame front, when the ratio of the fuel mixture to burnt gas density is unity $\Theta \equiv \rho_f/\rho_b=1$ [2,3]. In that case, a flame front propagates in a prescribed external turbulent flow without affecting the flow. However, in reality the expansion factor Θ is rather large, $\Theta=5-10$, and the flame interacts strongly with the flow, which leads to many additional phenomena such as the Darrieus-Landau (DL) instability [1,4]. As a matter of fact, attempts to simplify the whole system of combustion equations for a laminar flame with the expansion factor Θ different from unity have been usually coupled to the studies of the DL instability, see Ref. [5] as one of the latest reviews on the subject. The basic idea of the simplification is the following. A flame front is typically very thin in comparison with the hydrodynamic length scales, and it may be considered as a geometrical surface of zero thickness, separating fuel mixture and products of burning. In that case the solution to the combustion equations consists of three steps: (1) we have to solve equations of ideal hydrodynamics in the fuel mixture ahead of the flame front; (2) we have to solve equations of ideal hydrodynamics in the burnt matter behind the flame front; (3) we have to match the obtained solutions at the flame front with the help of conservation laws. If we succeed in these three steps of solution, then we find a single nonlinear equation of the front dynamics (or a set of equations), which contains only values and derivatives at the flame front but not in the bulk of the gas flow. In the case of a flame front of zero thickness, the matching conditions are specified by the conservation laws at a hydrodynamic discontinuity surface [6] plus the condition of constant velocity U_f of flame propagation with respect to the fuel mixture. However, the growth rate of the DL instability is not limited for a flame front of zero thickness, the evolution problem of an infinitely thin flame cannot be specified self-consistently, and we have to consider finite flame thickness [1,7]. Small but finite flame thickness may be taken into account as a parameter in the conservation laws at the flame front, which have been obtained in Refs. [7,8] for the linear approximation and in Ref. [9] for a strongly curved flame in the nonlinear regime. The respective formula for the local velocity of flame propagation depending on the flame stretch has been derived in Refs. [9,10]. The conservation laws specify step 3 in the above procedure. The solution to the hydrodynamic equations in the fuel mixture ahead of the flame front (step 1) is rather simple in the case of laminar burning, since ahead of the laminar flame the flow is potential no matter how corrugated is the front. The last and the most difficult part of the algorithm in the laminar case is to solve the hydrodynamic equations in the downstream flow behind the flame (step 2). Indeed, a curved flame front generates vorticity in the flow, which makes the flow essentially nonlinear [4,5]. If we consider turbulent burning, then the vorticity is nonzero both ahead of the flame front and behind the front, which makes the problem even more difficult. Therefore, trying to develop the model of a turbulent thin flame front, we have to solve first a similar laminar problem.

Up till now, the problem of laminar corrugated flame dynamics has been reduced to a single equation for the flame front position only under simplifying assumptions. Sivashinsky has derived an equation of this kind in the limit of small thermal expansion, $\Theta-1\ll 1$, assuming also weak nonlinearity of the flame front, i.e., a flame shape differs slightly from an ideally planar or ideally spherical front [11]. In the case of an arbitrary thermal expansion including realistically large expansion factors $\Theta=5-10$, an equation of flame front evolution has been derived in Ref. [12] using the same assumption of weak nonlinearity. The obtained equation described successfully the velocity of two-dimensional (2D) curved stationary flames [12,13] and the stability limits of the curved flames [14,15]. Unfortunately, the assumption of weak nonlinearity has rather limited number of applications, for example, it cannot be applied to the strongly nonlinear

fractal flames expected at large hydrodynamic length scales [5,16–18]. In order to describe fractal flames, we have to derive an equation (or a set of equations) at a flame front in a coordinate-free rotationally invariant form without any restriction on the nonlinear terms. Such an equation has been derived by Frankel [19] in the limit of small thermal expansion $\Theta-1\ll 1$, similar to the Sivashinsky equation (the Frankel equation may be reduced to the Sivashinsky equation for a weakly nonlinear front). The Frankel equation has been widely used [20–23] because it describes qualitatively the behavior of strongly corrugated flames. However, the limit of small thermal expansion, $\Theta-1\ll 1$, adopted by Frankel is too far from the parameters of realistic flames with the expansion factors $\Theta=5-10$ and cannot be utilized for a quantitative analysis. Therefore, what is needed is an equation (or a set of equations) at a discontinuous flame front, written in a coordinate-free form similar to the Frankel equation, but taking into account realistically large thermal expansion of the burning matter.

In the present paper, we reduce the complete set of hydrodynamic equations for a corrugated flame front to a system of coordinate-free equations at the front using the fact that the vorticity effects remain relatively weak even for a fractal flame. We demonstrate how small but finite flame thickness may be taken into account in the equations. We show that similar equations may be obtained for turbulent burning in the flamelet regime. The equations obtained for a turbulent corrugated flame are consistent with the Taylor hypothesis of ''stationary'' external turbulence.

II. BASIC EQUATIONS FOR AN INFINITELY THIN FLAME FRONT

We start with the DL approximation of an infinitely thin flame front. Assume that the gas dynamics of burning is characterized by a length scale R, which may be the radius of a tube, width of a channel, radius of a spherical burning chamber, etc. We introduce the dimensionless velocity of the flow scaled by the velocity of a planar flame front $\mathbf{u}=\mathbf{v}/U_f$, together with the scaled coordinates $\mathbf{r}=\mathbf{x}/R$, time $\tau=U_f t/R$, and pressure $\Pi=(P-P_f)/\rho_f U_f^2$, where ρ_f and P_f are density and pressure in the fuel mixture far ahead of the flame front. Within the framework of the DL approximation, the flame is treated as a discontinuity surface of zero thickness propagating at a constant velocity U_f relative to the fuel mixture. The flow is assumed to be incompressible and inviscid, and the hydrodynamic equations upstream and downstream of a corrugated flame take the form

$$\boldsymbol{\nabla}\cdot\mathbf{u}=0, \tag{1}$$

$$\frac{\partial\mathbf{u}}{\partial\tau}+(\mathbf{u}\cdot\boldsymbol{\nabla})\mathbf{u}=-\vartheta\boldsymbol{\nabla}\Pi, \tag{2}$$

where $\vartheta=1$ in the fuel mixture and $\vartheta=\Theta$ in the burnt gas. Let the flame front be described by the function

$$F(\mathbf{r},\tau)=0. \tag{3}$$

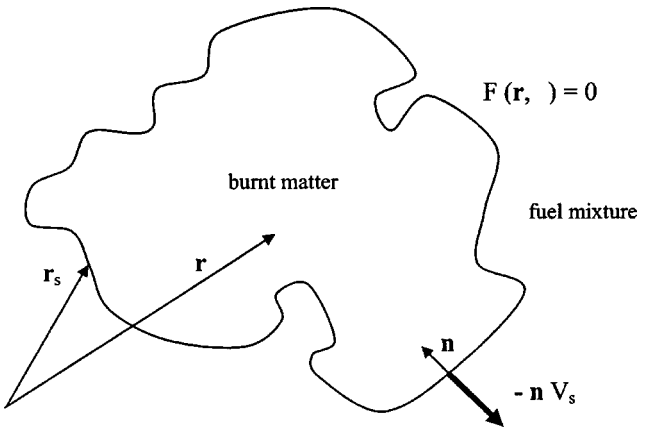

FIG. 1. Flame front propagating from a point of ignition.

We choose $F(\mathbf{r},\tau)<0$ in the fuel mixture and $F(\mathbf{r},\tau)>0$ in the products of burning, so that the normal unit vector $\mathbf{n}=\boldsymbol{\nabla}F/|\boldsymbol{\nabla}F|$ points to the products, see Fig. 1. The geometrical surface, $F(\mathbf{r},\tau)=0$, corresponding to the flame front propagates in the outward direction with velocity $-\mathbf{n}V_s$;

$$V_s=|\boldsymbol{\nabla}F|^{-1}\frac{\partial F}{\partial\tau}. \tag{4}$$

The jump conditions across an infinitely thin flame front are [6]

$$u_{n+}+V_s=\Theta(u_{n-}+V_s), \tag{5}$$

$$\mathbf{u}_{t+}=\mathbf{u}_{t-}, \tag{6}$$

$$\Pi_+ +\frac{1}{\Theta}(u_{n+}+V_s)^2=\Pi_- +(u_{n-}+V_s)^2. \tag{7}$$

Here labels ''$-$'' and ''$+$'' correspond to the positions just ahead of the flame front and just behind the front, while the labels n and t stand for the normal and the tangential directions. One more condition is that the flame front propagates at a fixed speed with respect to the fuel mixture,

$$u_{n-}+V_s=1. \tag{8}$$

Using Eq. (8), one can rewrite Eqs. (5)–(7) in the form

$$u_{n+}=u_{n-}+\Theta-1, \tag{9}$$

$$\mathbf{u}_+=\mathbf{u}_-+(\Theta-1)\mathbf{n}, \tag{10}$$

$$\Pi_+=\Pi_-+1-\Theta. \tag{11}$$

Equations (1) and (2) in the upstream and downstream flow together with the conditions at flame surface (8)–(11) describe the dynamics of an infinitely thin flame front.

Though the system [Eqs. (1), (2), and (8)–(11)] looks rather simple, in reality these equations are very difficult even for a numerical study because they require a solution in the bulk of a gas both ahead of the flame front and behind the flame. The purpose of the present paper is to reduce the

whole system [Eqs. (1), (2), and (8)–(11)] to a set of equations at the flame front, which is possible only under certain simplifying assumptions specified below.

III. THE APPROXIMATION OF SMALL VORTICITY IN THE FLOW OF THE BURNT MATTER BEHIND A CURVED FLAME FRONT

In this section, we discuss the simplifying assumptions, which can be used in describing the dynamics of corrugated flames. We start with the propagation of a curved laminar flame in a tube with boundary conditions of adiabatic walls and ideal slip at the walls. The advantage of such a geometry is that the shape of a curved flame front in a tube may be limited by only one stationary cell, which is easier for analysis than the fractal flame shape consisting of a large number of cells of different sizes imposed on each other [5,16]. According to the numerical simulations [13,15,24], a flame cell may be described as a cusp pointing to the burnt matter and a hump directed to the fresh fuel mixture. Taking into account the tube geometry, we choose scaled variables in the form $\mathbf{r}=(\mathbf{y},\xi)$, $\mathbf{u}=(\mathbf{w},v)$, where ξ is the coordinate axis along the walls. To be particular, we take the reference frame of a planar flame front, in which the fuel mixture at infinity moves towards the flame with velocity $\mathbf{u}=\mathbf{e}_\xi$. As we pointed out in the Introduction, we are interested first of all in the flow of the burning products. If the flame front is planar, then the velocity and pressure behind the flame are uniform $\mathbf{u}=\Theta\mathbf{e}_\xi$, $\Pi=-\Theta+1$ [12], but in the case of a curved flame the flow is different from the uniform one. Velocity deviation from the planar flow in the products of burning, $\tilde{\mathbf{u}}=\mathbf{u}-\Theta\mathbf{e}_\xi$, satisfies the equation

$$\frac{\partial\tilde{\mathbf{u}}}{\partial\tau}+\Theta\frac{\partial\tilde{\mathbf{u}}}{\partial\xi}+(\tilde{\mathbf{u}}\cdot\boldsymbol{\nabla})\tilde{\mathbf{u}}+\Theta\boldsymbol{\nabla}\Pi=0. \tag{12}$$

Equation (12) may be also presented in the form

$$\frac{\partial\tilde{\mathbf{u}}}{\partial\tau}+\Theta\frac{\partial\tilde{\mathbf{u}}}{\partial\xi}-\tilde{\mathbf{u}}\times\omega+\boldsymbol{\nabla}\left(\frac{\tilde{u}^2}{2}+\Theta\Pi\right)=0 \tag{13}$$

or

$$\left(\frac{\partial}{\partial\tau}+\Theta\frac{\partial}{\partial\xi}\right)\boldsymbol{\nabla}\times\tilde{\mathbf{u}}-\boldsymbol{\nabla}\times(\tilde{\mathbf{u}}\times\omega)=0, \tag{14}$$

where $\omega=\boldsymbol{\nabla}\times\mathbf{u}$ denotes vorticity [6]. The characteristic flow behind a curved flame cell obtained in the numerical simulations [13] is shown in Fig. 2. An important point about Fig. 2 is that, in spite of the curved flame shape, the main velocity component in the flow of the burnt matter is determined by the uniform drift velocity $\Theta\mathbf{e}_\xi$, while the velocity deviation from the uniform flow is rather weak, $\tilde{u}\ll\Theta$. According to Ref. [12], the relative role of the velocity deviation may be estimated as $\tilde{u}/\Theta\propto f/\lambda$, where f and λ are the characteristic amplitude and width of the flame cell. Direct numerical simulations of the flame dynamics show that the amplitude of one cell of a curved flame is rather small, $f/\lambda=0.25-0.35$, even for realistically large thermal expansion,

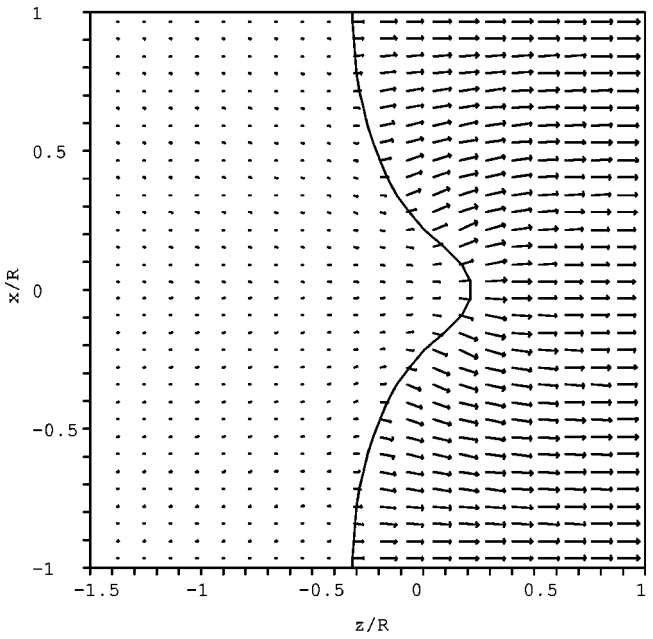

FIG. 2. Characteristic velocity field behind a curved flame front.

$\Theta=5-10$, both for 2D and 3D geometry [13,15,24]. Actually, this small curvature of the flame front is the reason why the analytical theory developed in the limit of weak nonlinearity is so successful in describing the dynamics of a single flame cell [12,14]. The relative role of vorticity in the flow of burning products may be specified by the combination $\omega\lambda/\Theta$. It was shown in Ref. [12] that the vorticity effects behind a curved flame front are as small as $\omega\lambda/\Theta\propto(f/\lambda)^2$. The secondary role of vorticity in the DL instability has been discussed for a long time [11,19,22]. Particularly, it has been demonstrated in Ref. [11] that vorticity is just a by-product of the DL instability, which may be neglected completely for small thermal expansion, $\Theta-1\ll1$. The assumption of zero vorticity in the burnt matter was the basis of the Frankel equation [19]. However, neglecting the vorticity in the burnt gas for realistically large expansion factors $\Theta=5-10$, one comes to an incorrect dispersion relation at the linear stage of the DL instability. Therefore in the present paper we take vorticity into account in the linear approximation. We propose to neglect the last term of Eq. (14), namely $\tilde{\mathbf{u}}\times\omega$, which stands for the nonlinear coupling between the flame-generated vorticity and the small deviation of the flow velocity from the drift velocity. According to the above estimates, the role of this nonlinear term is as small as $|\tilde{\mathbf{u}}\times\omega|\lambda/\Theta^2\propto(f/\lambda)^3=0.01-0.04$, which is definitely beyond the computational accuracy of the direct numerical simulations [13,15,24]. Using such an approximation (below we will call it the approximation of small vorticity), we reproduce correctly the linear dispersion relation of the DL instability for any expansion factor of the burning matter. Indeed, in that case Eq. (14) becomes

$$\left(\frac{\partial}{\partial\tau}+\Theta\frac{\partial}{\partial\xi}\right)\boldsymbol{\nabla}\times\tilde{\mathbf{u}}=\mathbf{0}, \tag{15}$$

with the solutions corresponding to the mode of vorticity drift,

$$\left(\frac{\partial}{\partial\tau}+\Theta\frac{\partial}{\partial\xi}\right)\tilde{\mathbf{u}}_v=\mathbf{0}, \tag{16}$$

and to the potential mode $\nabla\times\tilde{\mathbf{u}}_p=\mathbf{0}$, $\nabla^2\tilde{\mathbf{u}}_p=0$ with

$$\tilde{v}_p=\frac{1}{4\pi^2}\int \tilde{v}_{pk}\exp(-k\xi+i\mathbf{k}\cdot\mathbf{y})d^2k, \tag{17}$$

$$\tilde{\mathbf{w}}_p=-\hat{\Phi}^{-1}\nabla_\perp\tilde{v}_p. \tag{18}$$

Here $\hat{\Phi}$ stands for the DL operator,

$$\hat{\Phi}F=\frac{1}{4\pi^2}\int kF_k\exp(i\mathbf{k}\cdot\mathbf{y})d^2k, \tag{19}$$

where F_k is the Fourier transform of F, and $\nabla_\perp$ corresponds to the ∇ component in the plane perpendicular to the walls. One more important property of the potential mode is

$$\left(\frac{\partial}{\partial\tau}+\Theta\frac{\partial}{\partial\xi}\right)\tilde{\mathbf{u}}_p+\nabla\left(\frac{\tilde{u}^2}{2}+\Theta\Pi\right)=0, \tag{20}$$

which means that the dynamical pressure, $\tilde{u}^2/2+\Theta\Pi$, satisfies the Laplace equation in the burnt matter,

$$\nabla^2\left(\frac{\tilde{u}^2}{2}+\Theta\Pi\right)=0. \tag{21}$$

Obviously, the dynamical pressure obeys the Laplace equation in the fuel mixture ahead of the flame front too because the flow in the fuel mixture is potential. The solution to Eq. (15) in the fuel mixture is

$$v=1+\tilde{v}=1+\frac{1}{4\pi^2}\int \tilde{v}_k\exp(k\xi+i\mathbf{k}\cdot\mathbf{y})d^2k, \tag{22}$$

$$\mathbf{w}=\hat{\Phi}^{-1}\nabla_\perp\tilde{v}, \tag{23}$$

$$\Pi=\frac{1}{2}-\hat{\Phi}^{-1}\frac{\partial v}{\partial\tau}-\frac{\tilde{u}^2}{2}. \tag{24}$$

Taking matching conditions (10), (11) at a flame front, $F(\mathbf{r},\tau)=\xi-f(\mathbf{y},\tau)=0$, in the linear approximation

$$\tilde{v}_+=\tilde{v}_-,\quad \mathbf{w}_+=\mathbf{w}_--(\Theta-1)\nabla_\perp f,\quad \tilde{v}_-=\frac{\partial f}{\partial\tau} \tag{25}$$

and substituting the modes (16)–(18), (22)–(24), we come to the equation for the flame front perturbations,

$$(\Theta+1)\frac{\partial^2 f}{\partial\tau^2}+2\Theta\hat{\Phi}\frac{\partial f}{\partial\tau}-\Theta(\Theta-1)\hat{\Phi}^2 f=0, \tag{26}$$

which reproduces correctly the DL dispersion relation for any thermal expansion including the realistically large expansion factors $\Theta=5-10$ [6]. It is important that we do not neglect the mode of vorticity drift $\mathbf{u}_v$ in the burnt matter behind a corrugated flame front, but instead we neglect only the nonlinear coupling between the potential mode and the vorticity mode. Neglecting vorticity completely similar to Refs. [11,19,22], we would come to another dispersion relation

$$\frac{\partial f}{\partial\tau}-\frac{\Theta-1}{2}\hat{\Phi}f=0, \tag{27}$$

which holds only in the limit of small thermal expansion $\Theta-1\ll 1$. For realistically large expansion factors $\Theta=5-10$, dispersion relation (27) provides only qualitative, but not quantitative description of the DL instability. On the contrary, the present approximation of small but nonzero vorticity allows both the qualitative and the quantitative studies of the flame instability.

Taking into account the nonlinear corrections to Eqs. (25) and (26) in the limit of weak nonlinearity $(\nabla_\perp f)^2\ll 1$, we can demonstrate that the approximation of small vorticity describes well the propagation velocity of curved stationary flames and stability limits of these flames. As a matter of fact, in that case we just have to reproduce the calculations of Refs. [12,14], which is a long, but straightforward, procedure. A much subtler question is if the approximation of small vorticity can describe properly the dynamics of strongly corrugated fractal flames. A fractal structure implies the self-similar properties of a flame front at different length scales [5,16,17]. Because of the self-similarity every large cell at a flame front reproduces the shape of small cells like those observed for the flames propagating in relatively narrow tubes [13,15,24]. Then the characteristic ratio f/λ remains small for any cell of the fractal cascade, and the nonlinear effects related to the flame-generated vorticity may be neglected even for strongly corrugated fractal flames.

IV. COORDINATE-FREE EQUATION AT A FLAME FRONT OF ZERO THICKNESS

In the present section, we derive coordinate-free equations at a flame front of zero thickness ignited at a point. Taking into account the approximation of small vorticity, in the laboratory reference frame, we can write Eq. (2) in the form

$$\frac{\partial\mathbf{u}}{\partial\tau}+\nabla p=\mathbf{0}, \tag{28}$$

where $p=\vartheta\Pi+u^2/2$ is the dynamic pressure. All variables at the flame front (e.g., $\mathbf{u}_-$, $\mathbf{u}_+$, V_s, etc.) depend on time and on the coordinate along the front $\mathbf{r}_s$, see Fig. 1. Respective derivatives in space ∇_s coincide with the tangential derivative along the flame front, $\nabla_s=\mathbf{e}_t\cdot\nabla$, but the time derivative is related to the normal derivative in space,

$$\frac{\partial}{\partial\tau_s}=\frac{\partial}{\partial\tau}-V_s\frac{\partial}{\partial\mathbf{n}}, \tag{29}$$

since the flame front propagates locally with the velocity $-\mathbf{n}V_s$. The velocity field ahead of the flame front is potential, $\mathbf{u}=\boldsymbol{\nabla}\phi$, $\nabla^2\phi=0$, which leads to the Bernoulli integral

$$\frac{\partial\phi}{\partial\tau}+p=0, \tag{30}$$

taking the form

$$\frac{\partial\phi_-}{\partial\tau_s}+V_s u_{n-}+p_-=0 \tag{31}$$

exactly at the flame front. The velocity field behind the flame may be presented as a combination of a potential mode and a vorticity mode $\mathbf{u}=\mathbf{u}_p+\mathbf{u}_v$, satisfying the equations $\mathbf{u}_p=\boldsymbol{\nabla}\phi$, $\nabla^2\phi=0$, and

$$\frac{\partial\mathbf{u}_v}{\partial\tau}=\mathbf{0}. \tag{32}$$

It is interesting to note that the vorticity mode is time independent in the approximation of small vorticity similar to the well-known solution of the DL instability at a spherical flame propagating outwards from a point of ignition [26]. Taking into account Eq. (29), the last property may be also presented as

$$\frac{\partial\mathbf{u}_v}{\partial\tau_s}=-V_s\frac{\partial\mathbf{u}_v}{\partial\mathbf{n}}. \tag{33}$$

The respective Bernoulli integral at the flame front in the burnt matter is

$$\frac{\partial\phi_+}{\partial\tau_s}+V_s u_{pn+}+p_+=\text{const}. \tag{34}$$

Taking into account that the velocity potential is defined with the accuracy of a time-dependent function [6], we may drop the constant in the last equation. The boundary conditions for the velocity potentials at the flame front follow from Eqs. (8) and (9),

$$\frac{\partial\phi_-}{\partial\mathbf{n}}=u_{n-}=1-V_s, \tag{35}$$

$$\frac{\partial\phi_+}{\partial\mathbf{n}}=u_{pn+}=\Theta-V_s-u_{vn+}. \tag{36}$$

According to the Green solution to the Laplace equation, a harmonic function $\nabla^2\phi=0$ at a point $\mathbf{r}$ of a domain G with a surface S and a normal unit vector $\mathbf{n}_{out}$ pointing outwards may be found using the boundary conditions at the surface,

$$\beta\phi(\mathbf{r})=\int\int_S\left[\frac{1}{|\mathbf{r}_s-\mathbf{r}|}\frac{\partial\phi(\mathbf{r}_s)}{\partial\mathbf{n}_{out}}+\phi(\mathbf{r}_s)\mathbf{n}_{out}\cdot\frac{\mathbf{r}_s-\mathbf{r}}{|\mathbf{r}_s-\mathbf{r}|^3}\right]dS(\mathbf{r}_s), \tag{37}$$

where $\beta=4\pi$ if $\mathbf{r}$ is inside G, $\beta=2\pi$ if $\mathbf{r}$ is on the surface S, and $\beta=0$ if $\mathbf{r}$ is outside G. Then potentials ϕ_-, ϕ_+ at the flame front satisfy the following equations:

$$\phi_-(\mathbf{r})=\frac{1}{2\pi}\int\int_S\left[\frac{1-V_s}{|\mathbf{r}_s-\mathbf{r}|}+\phi_-\mathbf{n}\cdot\frac{\mathbf{r}_s-\mathbf{r}}{|\mathbf{r}_s-\mathbf{r}|^3}\right]dS(\mathbf{r}_s), \tag{38}$$

$$\phi_+(\mathbf{r})=-\frac{1}{2\pi}\int\int_S\left[\frac{\Theta-V_s-u_{vn+}}{|\mathbf{r}_s-\mathbf{r}|}+\phi_+\mathbf{n}\cdot\frac{\mathbf{r}_s-\mathbf{r}}{|\mathbf{r}_s-\mathbf{r}|^3}\right]dS(\mathbf{r}_s), \tag{39}$$

where all the values under the integrals depend on $\mathbf{r}_s$ (except for $\mathbf{r}$, of course). Equations (38) and (39) are integral equations, which determine the velocity potentials at the flame front, if the vorticity component of the velocity field is known just behind the flame. Therefore, we have to find the relation between the potential modes and the vorticity mode at the flame front. For that purpose, we write the continuity equation (1) for the vorticity mode in the form

$$\frac{\partial u_{vn+}}{\partial\mathbf{n}}+\boldsymbol{\nabla}_s\cdot\mathbf{u}_{vt+}=0, \tag{40}$$

and using Eq. (33) we reduce it to

$$\frac{\partial u_{vn+}}{\partial\tau_s}=V_s\boldsymbol{\nabla}_s\cdot\mathbf{u}_{vt+}. \tag{41}$$

The jump condition for the tangential velocity $\mathbf{u}_{t-}=\mathbf{u}_{t+}$, [Eq. (6)], leads to $\mathbf{u}_{t-}-\mathbf{u}_{pt+}=\mathbf{u}_{vt+}$ and couples the tangential velocity component of the vorticity mode and the velocity potentials as

$$\boldsymbol{\nabla}_s(\phi_--\phi_+)=\mathbf{u}_{vt+}. \tag{42}$$

Then, taking into account Eq. (41) we find the desired relation between the potential modes and the normal velocity component of the vorticity mode used in Eq. (39):

$$\frac{\partial u_{vn+}}{\partial\tau_s}=V_s\boldsymbol{\nabla}_s^2(\phi_--\phi_+). \tag{43}$$

Finally, we have to couple the potentials. For that purpose, we substitute Eqs. (31) and (34) into the condition of pressure jump at the flame front (11),

$$\frac{\partial}{\partial\tau_s}(\phi_+-\Theta\phi_-)=\Theta(\Theta-1)-\frac{u_+^2}{2}+\Theta\frac{u_-^2}{2}-V_s u_{n+}+V_s u_{vn+}+\Theta V_s u_{n-}. \tag{44}$$

Using Eqs. (8)–(10), we can reduce Eq. (44) to

$$\frac{\partial}{\partial\tau_s}(\phi_+ - \Theta\phi_-) = \frac{\Theta-1}{2}u_-^2 - (\Theta-1)V_s^2 + (\Theta-1)V_s + V_s u_{vn+} + \frac{(\Theta-1)^2}{2}. \quad (45)$$

Introducing the designations

$$\Psi = \frac{\phi_+ - \Theta\phi_-}{\Theta-1}, \quad \Omega = \frac{u_{vn+}}{\Theta-1}, \quad (46)$$

we can rewrite the final set of equations at the flame front in the form

$$\phi_-(\mathbf{r}) = \frac{1}{2\pi}\int\int_S \left[\frac{1-V_s}{|\mathbf{r}_s-\mathbf{r}|} + \phi_- \mathbf{n}\cdot\frac{\mathbf{r}_s-\mathbf{r}}{|\mathbf{r}_s-\mathbf{r}|^3}\right] dS(\mathbf{r}_s), \quad (47)$$

$$\Psi(\mathbf{r}) + \frac{\Theta+1}{\Theta-1}\phi_-(\mathbf{r}) = \frac{1}{2\pi}\int\int_S \left[\frac{\Omega-1}{|\mathbf{r}_s-\mathbf{r}|} - (\Psi+\phi_-)\mathbf{n}\cdot\frac{\mathbf{r}_s-\mathbf{r}}{|\mathbf{r}_s-\mathbf{r}|^3}\right] dS(\mathbf{r}_s), \quad (48)$$

$$\frac{\partial\Omega}{\partial\tau_s} = -V_s\nabla_s^2(\phi_- + \Psi), \quad (49)$$

$$\frac{\partial\Psi}{\partial\tau_s} = \frac{1}{2}u_-^2 - V_s^2 + (1+\Omega)V_s + \frac{\Theta-1}{2}. \quad (50)$$

Besides, velocity just ahead of the flame front is determined from Eq. (37) as

$$\mathbf{u}_-(\mathbf{r}) = \frac{1}{4\pi}\int\int_S \left[(1-V_s)\frac{\mathbf{r}_s-\mathbf{r}}{|\mathbf{r}_s-\mathbf{r}|^3} - \phi_-\frac{\partial}{\partial\mathbf{n}}\left(\frac{\mathbf{r}_s-\mathbf{r}}{|\mathbf{r}_s-\mathbf{r}|^3}\right)\right] dS(\mathbf{r}_s). \quad (51)$$

Then the flame front velocity may be calculated as $V_s = u_{n-} - 1$ [Eq. (8)], using Eq. (51). The system of Eqs. (47)–(51) contains only values and variables at the flame front, thus reducing the 3D problem [Eqs. (1), (2), (8)–(11)] in the bulk of the gas flow to a 2D problem of the flame dynamics as a discontinuity surface.

The system of Eqs. (47)–(51) holds for any thermal expansion of the burning matter including the realistic expansion factors $\Theta = 5-10$, when the corrugated flame shape generates vorticity behind the flame front. It is interesting to compare the above equations to the Frankel equation [19] obtained under the assumption of a potential flow in the burnt matter. As is known, the flow of the burnt gas may be treated as potential in the case of small thermal expansion, $\Theta - 1 \ll 1$ [11]. In that case, Eq. (49) takes the form of the Laplace equation on a closed surface $\nabla_s^2(\phi_- + \Psi) = 0$, which has the only solution $\phi_- + \Psi = \text{const}$. Since the potential of a double layer with constant density is also constant, then, in agreement with Ref. [19], Eq. (48) reduces to the velocity potential of a single layer,

$$\phi_-(\mathbf{r}) = -\frac{\Theta-1}{4\pi}\int\int_S \frac{dS(\mathbf{r}_s)}{|\mathbf{r}_s-\mathbf{r}|} + \text{const}. \quad (52)$$

Then after calculations, similar to Ref. [19], we come to the Frankel equation

$$V_s - 1 = -u_{n-} = \frac{\Theta-1}{2}\left[1 - \frac{1}{2\pi}\int\int_S \frac{\partial}{\partial\mathbf{n}}\frac{1}{|\mathbf{r}_s-\mathbf{r}|}dS(\mathbf{r}_s)\right]. \quad (53)$$

Equation (53) may be also reduced to the Sivashinsky equation [11] in the case of weak nonlinearity, see Ref. [19].

An interesting feature of Eqs. (47)–(51) is that the system obtained involves indirectly the second-order derivative in time, contrary to the Sivashinsky and Frankel equations which are only of the first order. The difference between the equations of the second and the first order in time may be crucial in the description of phenomena such as "tulip flames" [27] and flame-shock interaction [28,29].

V. EQUATIONS AT A FLAME FRONT OF FINITE THICKNESS

In the preceding section we have considered equations at an infinitely thin flame front. However, according to the DL theory, the instability growth rate of small perturbations at a flame front is infinitely large if the perturbation wavelength is not limited from below by the cut off wavelength $\Lambda_c = \lambda_c/R$ (proportional to the finite flame thickness). In order to describe the thermal stabilization of the DL instability one has to take into account the finite flame thickness in the conservation laws (5)–(7) [9]. Rigorous consideration of the finite flame thickness in Eqs. (5)–(7) requires rather long calculations and will be presented elsewhere. In the present section, we demonstrate how the effects of the thermal stabilization may be taken into account in the system [Eqs. (47)–(51)] in a simplified way similar to the classical Markstein approach [30]. For that purpose, we can observe that the development of the DL instability at both linear and nonlinear stages involves only one parameter of length dimension, namely the cutoff wavelength λ_c [9,12–14]. Similar to the Markstein approach, we take Eq. (8) in the form

$$u_{n-}+V_s=1-\Lambda Y, \tag{54}$$

where Y is stretch of the flame front (relative increase of the elementary surface area Δ at the flame front per unit time, $Y\equiv\Delta^{-1}d\Delta/d\tau_s$ [31]) and Λ is a coefficient characterizing the thermal stabilization of the DL instability. Other conservation laws (9)–(11) are considered without any change. We are going to find the relation between Λ and Λ_c and use Λ_c instead of Λ. In the linear case of a slightly perturbed flame front propagating in a tube, stretch may be calculated as [9]

$$Y=\boldsymbol{\nabla}_\perp\cdot\mathbf{w}_-+\nabla_\perp^2 f, \tag{55}$$

and one has to replace the last equation of Eq. (25) by

$$\frac{\partial f}{\partial\tau}-\tilde{v}_-=\Lambda(\boldsymbol{\nabla}_\perp\cdot\mathbf{w}_-+\nabla_\perp^2 f). \tag{56}$$

Then the system [Eqs. (16)–(18), (22)–(25), (56)] reduces to the dispersion equation

$$(\Theta+1)\frac{\partial^2 f}{\partial\tau^2}+2\Theta\left[1+\Lambda\frac{\Theta+1}{2\Theta}\hat{\Phi}\right]\hat{\Phi}\frac{\partial f}{\partial\tau}-\Theta(\Theta-1)\left[1-\Lambda\frac{\Theta+1}{\Theta-1}\hat{\Phi}\right]\hat{\Phi}^2 f=0. \tag{57}$$

As we can see from Eq. (57), the DL instability is stabilized at the perturbation wave number k_c, satisfying

$$1-\Lambda k_c\frac{\Theta+1}{\Theta-1}=0, \tag{58}$$

which corresponds to the cutoff wavelength $\Lambda_c=2\pi/k_c$, that is,

$$\Lambda=\frac{1}{2\pi}\frac{\Theta-1}{\Theta+1}\Lambda_c. \tag{59}$$

Thus Eq. (54) takes the form

$$u_{n-}+V_s=1-\frac{1}{2\pi}\frac{\Theta-1}{\Theta+1}\Lambda_c Y, \tag{60}$$

where $\Lambda_c=\lambda_c/R$ is the scaled cutoff wavelength of the DL instability (the dimensional value of the cutoff wavelength $\lambda_c=\Lambda_c R$ may be measured experimentally [32]).

Taking into account the stretch effects, we find the following boundary conditions for the velocity potential:

$$\frac{\partial\phi_-}{\partial\mathbf{n}}=u_{n-}=1-V_s-\Lambda Y, \tag{61}$$

$$\frac{\partial\phi_+}{\partial\mathbf{n}}=u_{pn+}=\Theta-V_s-\Theta\Lambda Y-u_{vn+}, \tag{62}$$

and the solution to the Laplace equation at the flame front,

$$\phi_-(\mathbf{r})=\frac{1}{2\pi}\int\int_S\left[\frac{1-V_s-\Lambda Y}{|\mathbf{r}_s-\mathbf{r}|}+\phi_-\mathbf{n}\cdot\frac{\mathbf{r}_s-\mathbf{r}}{|\mathbf{r}_s-\mathbf{r}|^3}\right]dS(\mathbf{r}_s), \tag{63}$$

$$\phi_+(\mathbf{r})=-\frac{1}{2\pi}\int\int_S\left[\frac{\Theta-V_s-\Theta\Lambda Y-u_{vn+}}{|\mathbf{r}_s-\mathbf{r}|}+\phi_+\mathbf{n}\cdot\frac{\mathbf{r}_s-\mathbf{r}}{|\mathbf{r}_s-\mathbf{r}|^3}\right]dS(\mathbf{r}_s). \tag{64}$$

The relation (43) is not affected by the finite flame stretch, but Eq. (45) is reduces to

$$\frac{\partial}{\partial\tau_s}(\phi_+-\Theta\phi_-)=\frac{\Theta-1}{2}u_-^2-(\Theta-1)V_s^2+(\Theta-1)V_s+V_s u_{vn+}-(\Theta-1)(V_s+\Theta-1)\Lambda Y+\frac{(\Theta-1)^2}{2}[1+(\Lambda Y)^2]. \tag{65}$$

Then the final set of equations at the flame front takes the form

$$\phi_-(\mathbf{r})=\frac{1}{2\pi}\int\int_S\left[\frac{1}{|\mathbf{r}_s-\mathbf{r}|}\left(1-V_s-\frac{\Theta-1}{\Theta+1}\frac{\Lambda_c Y}{2\pi}\right)+\phi_-\mathbf{n}\cdot\frac{\mathbf{r}_s-\mathbf{r}}{|\mathbf{r}_s-\mathbf{r}|^3}\right]dS(\mathbf{r}_s), \tag{66}$$

$$\Psi(\mathbf{r})+\frac{\Theta+1}{\Theta-1}\phi_-(\mathbf{r})=\frac{1}{2\pi}\int\int_S\left[\frac{1}{|\mathbf{r}_s-\mathbf{r}|}\left(\Omega-1+\frac{\Theta-1}{\Theta+1}\frac{\Lambda_c Y}{2\pi}\right)-(\Psi+\phi_-)\mathbf{n}\cdot\frac{\mathbf{r}_s-\mathbf{r}}{|\mathbf{r}_s-\mathbf{r}|^3}\right]dS(\mathbf{r}_s), \tag{67}$$

$$\frac{\partial\Omega}{\partial\tau_s}=-V_s\nabla_s^2(\phi_-+\Psi), \tag{68}$$

$$\frac{\partial\Psi}{\partial\tau_s}=\frac{1}{2}u_-^2-V_s^2+(1+\Omega)V_s-\frac{\Theta-1}{\Theta+1}\frac{\Lambda_c Y}{2\pi}(V_s+\Theta-1)+\frac{\Theta-1}{2}\left[1+\left(\frac{\Theta-1}{\Theta+1}\frac{\Lambda_c Y}{2\pi}\right)^2\right]. \tag{69}$$

The scaled cutoff wavelength of the DL instability, Λ_c, is the only parameter of length dimension involved in Eqs. (66)–(69) and, obviously, Λ_c is the smallest length scale that has to be resolved in the numerical solution to the above equations.

VI. EQUATIONS AT A TURBULENT FLAME FRONT

In this section, we will show how external turbulence may be included into Eqs. (66)–(69) using the approximation of small vorticity both upstream and downstream the flame front. Small effects of vorticity in the flamelet regime of turbulent burning has been discussed recently in Refs. [21,22], where vorticity has been neglected completely. The approximation of the present paper is much less restrictive, though, of course, the accuracy of such an approximation is considerably lower for turbulent flames in comparison with the laminar ones because the vorticity effects are obviously stronger for turbulent flames. Still, the present approximation is consistent with the Taylor hypothesis of ''stationary'' turbulence [1], which follows from Eq. (28) applied to the turbulent flow of the fuel mixture. The Taylor hypothesis has not been proven rigorously, but it was used in the majority of papers devoted to turbulent burning in the flamelet regime, see, for example, Refs. [3,21,33]. The recent investigation of the flame dynamics in a flow with temporal pulsations of external turbulent velocity [34] has demonstrated that the Taylor hypothesis does provide a good model for the flamelet regime of burning.

In the case of turbulent flames, the upstream flow in the fuel mixture contains both a potential mode and a turbulent mode of vorticity drift $\mathbf{u}_e$, and the boundary condition for the velocity potential at the flame front is

$$\frac{\partial \phi_-}{\partial \mathbf{n}} = u_{pn-} = u_{n-} - u_{en-} = 1 - V_s - u_{en-} - \Lambda Y, \quad (70)$$

where u_{en-} is the normal component of the external turbulent velocity at the flame front, and the respective solution to the Laplace equation ahead of the front is

$$\phi_-(\mathbf{r}) = \frac{1}{2\pi}\int\int_S \left[\frac{1}{|\mathbf{r}_s-\mathbf{r}|}\left(1 - V_s - u_{en-} - \frac{\Theta-1}{\Theta+1}\,\frac{\Lambda_c Y}{2\pi}\right) + \phi_- \mathbf{n}\cdot\frac{\mathbf{r}_s-\mathbf{r}}{|\mathbf{r}_s-\mathbf{r}|^3}\right] dS(\mathbf{r}_s), \quad (71)$$

with the velocity in the fuel mixture at the flame front,

$$\mathbf{u}_- = \mathbf{u}_e + \frac{1}{4\pi}\int\int_S \left[\left(1 - V_s - u_{en-} - \frac{\Theta-1}{\Theta+1}\,\frac{\Lambda_c Y}{2\pi}\right)\frac{\mathbf{r}_s-\mathbf{r}}{|\mathbf{r}_s-\mathbf{r}|^3} - \phi_- \frac{\partial}{\partial \mathbf{n}}\left(\frac{\mathbf{r}_s-\mathbf{r}}{|\mathbf{r}_s-\mathbf{r}|^3}\right)\right] dS(\mathbf{r}_s). \quad (72)$$

The equation relating the vorticity modes and the potential modes at the flame front takes the form

$$\frac{\partial}{\partial \tau_s}(u_{vn+} - u_{en-}) = V_s \nabla_s^2 (\phi_- - \phi_+), \quad (73)$$

while the equation coupling two potential modes upstream and downstream the flame front coincides with Eq. (65). Then the final system of equations at a turbulent flame front is

$$\phi_-(\mathbf{r}) = \frac{1}{2\pi}\int\int_S \left[\frac{1}{|\mathbf{r}_s-\mathbf{r}|}\left(1 - V_s - u_{en-} - \frac{\Theta-1}{\Theta+1}\,\frac{\Lambda_c Y}{2\pi}\right) + \phi_- \mathbf{n}\cdot\frac{\mathbf{r}_s-\mathbf{r}}{|\mathbf{r}_s-\mathbf{r}|^3}\right] dS(\mathbf{r}_s), \quad (74)$$

$$\Psi(\mathbf{r}) + \frac{\Theta+1}{\Theta-1}\phi_-(\mathbf{r}) = \frac{1}{2\pi}\int\int_S \left[\frac{1}{|\mathbf{r}_s-\mathbf{r}|}\left(\Omega - \frac{u_{en-}}{\Theta-1} - 1 + \frac{\Theta-1}{\Theta+1}\,\frac{\Lambda_c Y}{2\pi}\right) - (\Psi + \phi_-)\mathbf{n}\cdot\frac{\mathbf{r}_s-\mathbf{r}}{|\mathbf{r}_s-\mathbf{r}|^3}\right] dS(\mathbf{r}_s), \quad (75)$$

$$\frac{\partial}{\partial \tau_s}\left(\Omega - \frac{u_{en-}}{\Theta-1}\right) = -V_s \nabla_s^2 (\phi_- + \Psi), \quad (76)$$

$$\frac{\partial \Psi}{\partial \tau_s} = \frac{1}{2}u_-^2 - V_s^2 + \left(1 - \frac{\Theta u_{en-}}{\Theta-1} + \Omega\right)V_s - \frac{\Theta-1}{\Theta+1}\,\frac{\Lambda_c Y}{2\pi}(V_s + \Theta - 1) + \frac{\Theta-1}{2}\left[1 + \left(\frac{\Theta-1}{\Theta+1}\,\frac{\Lambda_c Y}{2\pi}\right)^2\right]. \quad (77)$$

Of course, in reality the turbulent velocity field $\mathbf{u}_e$ at the flame front does not coincide with the velocity field far ahead of the flame front. However, the present knowledge about the initial ''free'' turbulence induced in gas turbines and car engines is very limited. Though the standard assumption about the external velocity field used in the numerical simulations [21,22,33,34] is the assumption of an isotropic Kolmogorov turbulence, one cannot say for sure that such a

turbulence takes place in combustion experiments [25,35,36] and in industrial energy production devices. Therefore, instead of making assumptions about turbulence far ahead of the flame front, at present one can make assumptions directly about the turbulent velocity field at the flame front.

VII. EQUATIONS AT A FLAME FRONT IN A TWO-DIMENSIONAL GEOMETRY

Though Eqs. (74)–(77) do reduce the hydrodynamic problem in the bulk of the gas flow to a set of equations at the flame front, the resulting system is still rather difficult for numerical solution. By this reason, it is natural to expect that the first modeling of Eqs. (74)–(77) will be performed in the 2D geometry rather than in the 3D one. In this section, we present the 2D version of the system [Eqs. (74)—(77)], for which the flame front is a corrugated loop instead of a surface. We start with the infinitely thin laminar flame. In that case, the integral expression for the Green solution to the Laplace equation (37) takes the form

$$\gamma\phi(\mathbf{r})=\int_S\left[\frac{\partial\phi(\mathbf{r}_s)}{\partial\mathbf{n}_{out}}\ln|\mathbf{r}_s-\mathbf{r}|-\phi(\mathbf{r}_s)\mathbf{n}_{out}\cdot\frac{\mathbf{r}_s-\mathbf{r}}{|\mathbf{r}_s-\mathbf{r}|^2}\right]dS(\mathbf{r}_s), \tag{78}$$

where the curve S is the boundary of a 2D domain G. The factor γ is zero ($\gamma=0$) if $\mathbf{r}$ is outside G, $\gamma=\pi$ if $\mathbf{r}$ belongs to the curve S, and $\gamma=2\pi$ if $\mathbf{r}$ is inside G. Therefore, at the flame front we have the following expressions for the velocity potentials:

$$\phi_+(\mathbf{r})=-\frac{1}{\pi}\int_S\left[(\Theta-V_s-u_{vn+})\ln|\mathbf{r}_s-\mathbf{r}|-\phi_+\mathbf{n}\cdot\frac{\mathbf{r}_s-\mathbf{r}}{|\mathbf{r}_s-\mathbf{r}|^2}\right]dS(\mathbf{r}_s), \tag{79}$$

$$\phi_-(\mathbf{r})=\frac{1}{\pi}\int_S\left[(1-V_s)\ln|\mathbf{r}_s-\mathbf{r}|-\phi_-\mathbf{n}\cdot\frac{\mathbf{r}_s-\mathbf{r}}{|\mathbf{r}_s-\mathbf{r}|^2}\right]dS(\mathbf{r}_s). \tag{80}$$

Equation (80) is the 2D counterpart of Eq. (47). The counterpart of Eq. (48) follows from Eqs. (79) and (80),

$$\Psi(\mathbf{r})+\frac{\Theta+1}{\Theta-1}\phi_-(\mathbf{r})=\frac{1}{\pi}\int_S\left[(\Omega-1)\ln|\mathbf{r}_s-\mathbf{r}|+(\Psi+\phi_-)\mathbf{n}\cdot\frac{\mathbf{r}_s-\mathbf{r}}{|\mathbf{r}_s-\mathbf{r}|^2}\right]dS(\mathbf{r}_s). \tag{81}$$

Equation (49) and (50) remain the same in the 2D geometry as they were in the 3D one,

$$\frac{\partial\Omega}{\partial\tau_s}=-V_s\nabla_s^2(\phi_-+\Psi), \tag{82}$$

$$\frac{\partial\Psi}{\partial\tau_s}=\frac{1}{2}u_-^2-V_s^2+(1+\Omega)V_s+\frac{\Theta-1}{2}, \tag{83}$$

and the velocity just ahead of the flame front may be found from Eq. (78):

$$\mathbf{u}_-(\mathbf{r})=\frac{1}{2\pi}\int_S\left[-(1-V_s)\frac{\mathbf{r}_s-\mathbf{r}}{|\mathbf{r}_s-\mathbf{r}|^2}+\phi_-\frac{\partial}{\partial\mathbf{n}}\left(\frac{\mathbf{r}_s-\mathbf{r}}{|\mathbf{r}_s-\mathbf{r}|^2}\right)\right]dS(\mathbf{r}_s). \tag{84}$$

The set of equations (80)–(84) presents a coordinate-free description of 2D laminar flames with infinitely small flame thickness. Similar to Secs. V and VI, we may take into account stretch effects (produced by finite flame thickness) and external turbulence. Then the system [Eqs. (80)–(84)] takes the form

$$\phi_-(\mathbf{r})=\frac{1}{\pi}\int_S\left[\left(1-V_s-u_{en-}-\frac{\Theta-1}{\Theta+1}\frac{\Lambda_cY}{2\pi}\right)\ln|\mathbf{r}_s-\mathbf{r}|-\phi_-\mathbf{n}\cdot\frac{\mathbf{r}_s-\mathbf{r}}{|\mathbf{r}_s-\mathbf{r}|^2}\right]dS(\mathbf{r}_s), \tag{85}$$

$$\Psi(\mathbf{r})+\frac{\Theta+1}{\Theta-1}\phi_-(\mathbf{r})=\frac{1}{\pi}\int_S\left[\left(\Omega-\frac{u_{en-}}{\Theta-1}-1+\frac{\Theta-1}{\Theta+1}\frac{\Lambda_cY}{2\pi}\right)\ln|\mathbf{r}_s-\mathbf{r}|+(\Psi+\phi_-)\mathbf{n}\cdot\frac{\mathbf{r}_s-\mathbf{r}}{|\mathbf{r}_s-\mathbf{r}|^2}\right]dS(\mathbf{r}_s), \tag{86}$$

$$\frac{\partial}{\partial\tau_s}\left(\Omega-\frac{u_{en-}}{\Theta-1}\right)=-V_s\nabla_s^2(\phi_-+\Psi), \tag{87}$$

$$\frac{\partial\Psi}{\partial\tau_s}=\frac{1}{2}u_-^2-V_s^2+\left(1-\frac{\Theta u_{en-}}{\Theta-1}+\Omega\right)V_s-\frac{\Theta-1}{\Theta+1}\frac{\Lambda_cY}{2\pi}(V_s+\Theta-1)+\frac{\Theta-1}{2}\left[1+\left(\frac{\Theta-1}{\Theta+1}\frac{\Lambda_cY}{2\pi}\right)^2\right], \tag{88}$$

$$\mathbf{u}_-(\mathbf{r}) = \mathbf{u}_e - \frac{1}{2\pi}\int_S \left[\left(1 - V_s - u_{en-} - \frac{\Theta - 1}{\Theta + 1}\frac{\Lambda_c Y}{2\pi} \right) \frac{\mathbf{r}_s - \mathbf{r}}{|\mathbf{r}_s - \mathbf{r}|^2} - \phi_- \frac{\partial}{\partial \mathbf{n}} \left(\frac{\mathbf{r}_s - \mathbf{r}}{|\mathbf{r}_s - \mathbf{r}|^2} \right) \right] dS(\mathbf{r}_s). \tag{89}$$

VIII. SUMMARY

In the present paper, we have reduced the whole system of hydrodynamic equations in the bulk of the gas flow ahead of a corrugated flame front and behind the front to a set of equations at the flame front; see Eqs. (47)—(50) for a laminar flame front of zero thickness, Eqs. (66)–(69) for a laminar flame front of finite thickness, and Eqs. (74)—(77) for a flame front in an external turbulent flow. The derived equations may provide considerable gain in the numerical simulations of laminar and turbulent corrugated flames in the flamelet regime. First, the derived equations reduce the dimension of the problem by one, since a 3D problem of the gas flow is replaced by a 2D problem of the flame front dynamics considered as a geometrical surface. Second, the smallest length scale involved in the equations, which has to be resolved in the numerical simulations, is the cutoff wavelength of the DL instability λ_c. This length scale is almost three orders of magnitude larger that the thickness of the reaction zone, which has to be resolved in the direct numerical simulations. Indeed, the thickness of the reaction zone with realistically large activation energy of the chemical reactions is usually about 0.1 of the flame thickness, see Refs. [13,15,24]. On the other hand, the cutoff wavelength typically exceeds the flame thickness by a factor of $40-50$ [7,37]. Thus the cutoff wavelength λ_c is larger than the thickness of the reaction zone by a factor of $400-500$.

With all these advantages of the obtained equations (74)–(77), one may hope to model turbulent burning in realistic energy production devices, for which the characteristic length scale of the hydrodynamic flow $(10-100)$ cm exceeds the thickness of the reaction zone by $5-6$ orders of magnitude, making these flows far beyond the reach of the direct numerical simulations. Still, as a next step of the research, the equations obtained have to be validated by comparing the numerical results of the model to the experiments and the direct numerical simulations. This will be the subject of the future work.

ACKNOWLEDGMENT

This work was supported by the Swedish Research Council (VR).

[1] F.A. Williams, *Combustion Theory* (Benjamin, CA, 1985).
[2] A.R. Kerstein, W.T. Ashurst, and F.A. Williams, Phys. Rev. A **37**, 2728 (1988).
[3] V. Yakhot, Combust. Sci. Technol. **60**, 191 (1988).
[4] Ya.B. Zeldovich, G.I. Barenblatt, V.B. Librovich, and G.M. Makhviladze, *The Mathematical Theory of Combustion and Explosion* (Consultants Bureau, New York, 1985).
[5] V.V. Bychkov and M.A. Liberman, Phys. Rep. **325**, 115 (2000).
[6] L.D. Landau and E.M. Lifshitz, *Fluid Mechanics* (Pergamon Press, Oxford, 1989).
[7] P. Pelce and P. Clavin, J. Fluid Mech. **124**, 219 (1982).
[8] P. Clavin and F.A. Williams, J. Fluid Mech. **116**, 251 (1982).
[9] M. Matalon and B. Matkowsky, J. Fluid Mech. **124**, 239 (1982).
[10] P. Clavin and G. Joulin, J. Phys. (France) Lett. **44**, L1 (1983).
[11] G.I. Sivashinsky, Acta Astronaut. **4**, 1177 (1977).
[12] V.V. Bychkov, Phys. Fluids **10**, 2091 (1998).
[13] V.V. Bychkov, S.M. Golberg, M.A. Liberman, and L.E. Eriksson, Phys. Rev. E **54**, 3713 (1996).
[14] V. Bychkov, K. Kovalev, and M. Liberman, Phys. Rev. E **60**, 2897 (1999).
[15] O.Yu. Travnikov, V.V. Bychkov, and M.A. Liberman, Phys. Rev. E **61**, 468 (2000).
[16] Y. Gostintsev, A. Istratov, and Y. Shulenin, Combust., Explos. Shock Waves **24**, 563 (1988).
[17] D. Bradley, T.M. Cresswell, and J.S. Puttock, Combust. Flame **124**, 551 (2001).
[18] R.C. Aldredge and B. Zuo, Combust. Flame **127**, 2091 (2001).
[19] M. Frankel, Phys. Fluids A **2**, 1879 (1990).
[20] S.I. Blinnikov and P.V. Sasorov, Phys. Rev. E **53**, 4827 (1996).
[21] B. Denet, Phys. Rev. E **55**, 6911 (1997).
[22] N. Peters, H. Wenzel, and F.A. Williams, in *Proceedings of the Twenty-Eighth Symposium on Combustion*, edited by C.K. Law *et al.* (The Combustion Institute, Pittsburgh, 2000), p. 235.
[23] B. Denet, Phys. Fluids **14**, 3577 (2002).
[24] S. Kadowaki, Phys. Fluids **11**, 3426 (1999).
[25] R.C. Aldredge, V. Vaezi, and P.D. Ronney, Combust. Flame **115**, 395 (1998).
[26] A.G. Istratov and V.B. Librovich, J. Appl. Math. Mech. **7**, 43 (1966).
[27] J. Dold and G. Joulin, Combust. Flame **100**, 450 (1995).
[28] V.V. Bychkov, Phys. Fluids **10**, 2669 (1998).
[29] O.Yu. Travnikov, V.V. Bychkov, and M.A. Liberman, Combust. Sci. Technol. **142**, 1 (1999).
[30] G.H. Markstein, *Nonsteady Flame Propagation* (Pergamon Press, Oxford, 1964).
[31] M. Matalon and B. Matkowsky, Combust. Sci. Technol. **34**, 295 (1983).
[32] C. Clanet and G. Searby, Phys. Rev. Lett. **80**, 3867 (1998).
[33] L. Kagan and G. Sivashinsky, Combust. Flame **120**, 222 (2000).
[34] V. Bychkov and B. Denet, Combust. Theory Modell. **6**, 209 (2002).

[35] R. Abdel-Gayed, D. Bradley, and M. Lawes, Proc. R. Soc. London, Ser. A **414**, 389 (1987).

[36] H. Kobayashi, Y. Kawabata, and K. Maruta, in *Proceedings of the Twenty-Seventh Symposium on Combustion*, edited by C.K. Law *et al.* (The Combustion Institute, Pittsburgh, 1998), p. 941.

[37] G. Searby and D. Rochweger, J. Fluid Mech. **231**, 529 (1991).